doi:10.1017/S1431927621001963
Microsc. Microanal. 27 (Suppl 1), 2021

Examining Partial Crystallization in the $Co_{(78-x)}Fe_2Mn_xB_{14}Si_2Nb_4$ Magnetic Amorphous Nanocomposite Alloy Series

Alicia Koenig[1], David Tweddle[1], Alex Leary[2], Ronald Noebe[2], Claudia Mewes[3], Tim Mewes[1] and Gregory Thompson[1]

[1]The University of Alabama, United States, [2]NASA Glenn Research Center, United States, [3]University of Alabama, United States

Significant effort is being made towards the reduction of size and weight of electrical motors, which can be achieved through the development of materials that improve electronic power conversion. Magnetic amorphous nanocomposites (MANCs) are such a class of materials. They are composed of small crystallites, typically a strongly ferromagnetic species, contained within an amorphous intergranular matrix. These alloys are melt spun forming an amorphous matrix ribbon from which annealing promotes partial crystallization. Both the composition of the ribbon and subsequent annealing conditions offers a rich processing window to tune the magnetic properties in achieving favorable performance under medium to high frequency magnetic field reversals while maintaining low losses [1].

Recent work in the $Co_{(78-x)}Fe_2Mn_xB_{14}Si_2Nb_4$ alloys (x = 0.5, 2.0, 4.0, and 6.0 at.%) has shown that the permeability of the alloy can be dramatically reduced with increasing Mn content [2]. To date, the influence of the Mn partitioning on the crystallization has not been elucidated. In this study, atom probe tomography has been used to quantify this chemical evolution for the above series of MANCs that have been annealed at 520°C for 20 minutes to promote this partial crystallization.

Evidence of short-range ordering has been shown in partially crystallized samples by applying the pair distribution function to TEM electron diffraction patterns [3]. This ordering is similar to that of crystalline HCP Co, per Figure 1. APT compositional analysis revealed a preference for the ferromagnetic elements, Fe and Co, to be in the crystalline phase, while B, Si, and Nb enriched the amorphous phase. The elements B and Si are glass forming elements and would contribute to the stabilization of the amorphous phase as well as increase the electrical resistivity of the matrix. The incorporation of the early transition metal, Nb, reduces the crystallite coarsening such that these features remain nanoscale where ferromagnetic exchange lengths exhibit low coercivity and variable permeability. The Mn element is also found to predominately reside in the amorphous phase. Of particular interest is that the Co content in the crystallite phase does not decrease with increasing Mn content, where the increase in Mn is offset by the decrease in Co.

Keeping all the APT field evaporation specimen shapes similar (radius of curvature, shank angle, etc.) between all alloys, we are able to compare changes in their reconstructed atom maps. Figure 1 are a series of 2D density slices revealing a clear increase in the density of the crystallite phase with increasing Mn content. This increase in density signifies an increase in crystallinity, which could account for the improved permeability. Recalling that the Co content is decreased with Mn, the B:Co ratio is altered. Belashchenko et al. [4] reported that a higher B:Co ratio promotes a higher vacancy formation in amorphous Co-B alloys. This increase in crystallinity may then be explained by such an increase in the vacancy point defect concentration associated changes in this B:Co ratio within our alloys. An increase in vacancies would promote the diffusivity of the partitioning between the species that would then facilitate an increase in crystallization and explain the chemical contributions towards the reported magnetic properties with Mn content.

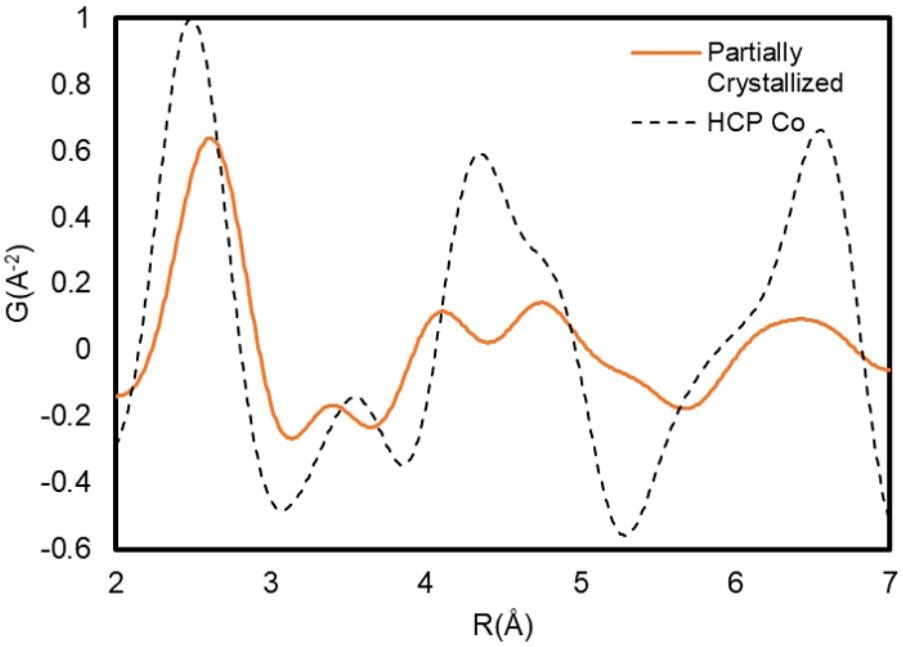

Figure 1. Pair distribution function (PDF) of partially crystallized Co72Fe2Mn6B14Si2Nb4 and simulated PDF of crystalline HCP Co.

https://doi.org/10.1017/S1431927621001963 Published online by Cambridge University Press

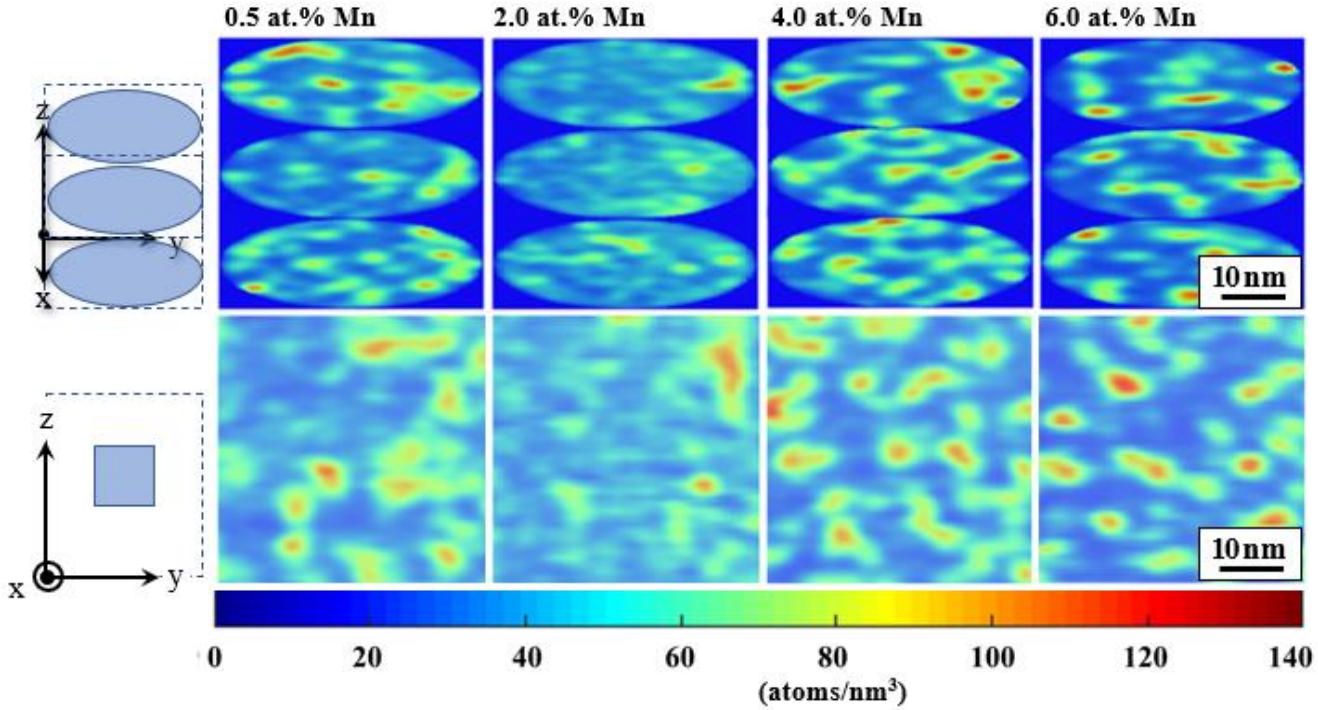

Figure 2. 2D density maps for each Co78-xFe2MnxNb4Si2B14 sample. Densities are in atoms/nm3 and have been corrected for detector efficiency.

References

[1] M. A. Bahmani, T. Thiringer, and M. Kharezy, "Design Methodology and Optimization of a Medium-Frequency Transformer for High-Power DC–DC Applications," *IEEE Trans. Ind. Appl.*, vol. 52, no. 5, pp. 4225–4233, Sep. 2016, doi: 10.1109/TIA.2016.2582825.

[2] A. Leary, V. Keylin, A. Devaraj, V. DeGeorge, P. Ohodnicki, and M. E. McHenry, "Stress induced anisotropy in Co-rich magnetic nanocomposites for inductive applications," *J. Mater. Res.*, vol. 31, no. 20, pp. 3089–3107, Oct. 2016, doi: 10.1557/jmr.2016.324.

[3] L. Khouchaf, K. Boulahya, P. P. Das, S. Nicolopoulos, V. K. Kis, and J. L. Lábár, "Study of the Microstructure of Amorphous Silica Nanostructures Using High-Resolution Electron Microscopy, Electron Energy Loss Spectroscopy, X-ray Powder Diffraction, and Electron Pair Distribution Function," *Mater. Basel Switz.*, vol. 13, no. 19, Oct. 2020, doi: 10.3390/ma13194393.

[4] D. K. Belashchenko, V. V. Hoang, and P. K. Hung, "Computer simulation of local structure and magnetic properties of amorphous Co–B alloys," *J. Non-Cryst. Solids*, vol. 276, no. 1, pp. 169–180, Oct. 2000, doi: 10.1016/S0022-3093(00)00262-3.

https://doi.org/10.1017/S1431927621001963 Published online by Cambridge University Press